A green method based on electro-assisted and photo-assisted regeneration for removal of chromium(VI) from aqueous solution

Jianyu Xing, Yu Shen, Bin Yang, Dongdong Feng, Wei Wang and Bo Bai

ABSTRACT

In general, spent adsorbent is regenerated using high-concentration chemicals. Although chemical regeneration is efficient, it often leads to adsorbent damage and secondary waste. To overcome these problems, electro-assisted and photo-assisted regeneration were proposed in this study for the remediation of hexavalent chromium (Cr(VI)). Filter paper was decorated with polyethylene glycol (PEG) and polypyrrole (PPy) to fabricate a FP/PEG/PPy nanocomposite, which could be used as an adsorbent for Cr(VI) with a high adsorption capacity. Moreover, it could be regenerated by electro-assisted or photo-assisted regeneration to reduce eluent use. As a result, secondary waste could be greatly reduced.

Key words | chromium (VI), conductive polymer, electro-assisted regeneration, photo-assisted regeneration

Jianyu Xing (corresponding author)
Yu Shen
Bin Yang
Dongdong Feng
Wei Wang
Bo Bai
School of Environmental Science and Engineering,
Chang'an University (Xi'an),
Shaanxi 710054,
China
E-mail: *xingjy@chd.edu.cn*

INTRODUCTION

Among various heavy metal pollutants, chromium (Cr) is one of the most toxic found in various industrial wastewaters (Dantas *et al.* 2001; Chiha *et al.* 2006; Aroua *et al.* 2007; Yusof & Malek 2009; Bhaumik *et al.* 2012). In general, chromium exists in nature in two valence states, hexavalent chromium (Cr(VI)) and trivalent chromium (Cr(III)). Cr(VI) is found to be more toxic than Cr(III) by the oral route (Wampler *et al.* 1996). Unfortunately, almost all Cr(VI) contamination comes from human activities (Bermúdez *et al.* 2012). The main source of contamination is the effluents from the chrome plating and leather tanning industries. Concern regarding exposure to Cr(VI) has been growing in recent years. According to the guidelines of the World Health Organization (WHO) and the United States Environmental Protection Agency (US EPA), the maximum permissible concentration of total Cr in industrial wastewater discharge is 0.1 mg/L, while that in drinking water should be less than 0.05 mg/L (Chiha *et al.* 2006). Therefore, the removal of chromium or the reduction of Cr(VI) to Cr(III) is the main route for the remediation of chromium pollution.

Adsorption is a commonly used method in the treatment of chromium pollution. Different types of adsorbent materials have been widely assessed, such as activated carbon (Pérez-Candela *et al.* 1995), metal oxide (Goshu *et al.* 2009), activated alumina (Bishnoi *et al.* 2004), coated silica gel (Gang *et al.* 2001), biomaterials (Levankumar *et al.* 2009) and conducting polymers. Although the efficient and high-capacity adsorption of Cr(VI) can be achieved by fabricating nanomaterials, the desorption process still occurs by the traditional chemical route. As a result, the desorption process not only affects the life of the adsorbent but also causes more secondary pollution. To reduce the requirement of chemical reagents in the desorption process, conductive polymers are increasingly recognized as being useful (Xing *et al.* 2018). Among all adsorption materials, conducting polymers, such as polythiophene (PT), polypyrrole (PPy) and polyaniline (PANI), are unique. In addition to their advantages of low cost, low toxicity, and chemical and physical stability, the greatest advantages of conductive polymers are their workability, conductivity and photoactivity. Conducting polymers have therefore become important media for the removal of heavy metals from aqueous solutions.

PPy, as a representative conducting polymer, has been used as an adsorbent for Pb(II), Cd(II) (Karthik & Meenakshi 2015), Cr(VI) (Bhaumik *et al.* 2012), Cu(II) (Ghorbani & Eisazadeh 2013), Zn(II) (Omraei *et al.* 2011), and Hg(II) (Lim *et al.* 2012). Based on the conductivity of PPy, electrically switched ion exchange technology (ESIX) has been

doi: 10.2166/wst.2018.260

proposed (Zhang *et al.* 2011; Choi *et al.* 2017; Xing *et al.* 2018). In a typical ESIX process, anion uptake occurs when oxidation of the PPy is performed by applying a positive potential, which forces the anions from the waste solution into the film. Elution is performed by applying a negative potential, which forces the anions out of the film and into the elution solution. This technology greatly reduces the dependence on elution reagents and improves the efficiency of the elution. It has been reported that PPy-based materials have photo-adsorption properties that can lead to thermal changes. (Huang *et al.* 2017). The desorption process in ESIX is a simple diffusion process which, if enhanced by increasing temperature, is beneficial for Cr(VI) removal and the regeneration of the adsorbent. Moreover, PPy can absorb light and produce photoinduced electron and hole pairs, which may benefit the remediation of Cr(VI) (Rammelt *et al.* 1999; Chowdhury *et al.* 2005).

In traditional desorption processes, the adsorbent plays a passive role, and a high concentration of eluent is necessary for the exchange of Cr(VI) (Ballav *et al.* 2012; Zhao *et al.* 2015). Based on the above analysis, the dedoping process induced by electrical conductivity and the thermal diffusion process induced by photoadsorption are all conducive to the regeneration of adsorbent. That means the adsorbent can be more active in the desorption process. In this paper, filter paper (FP) was modified with polyethylene glycol (PEG) and PPy to fabricate a FP/PEG/PPy composite for the removal of Cr(VI) in aqueous solution. Electro-assisted and photo-assisted desorption were evaluated for the removal of Cr(VI). It is expected that the FP/PEG/PPy composite can achieve green regeneration while attaining a high adsorption capacity.

EXPERIMENT

Materials

All starting materials, including FP, PEG, ferric chloride, hydrochloric acid and potassium dichromate, were obtained commercially and were used as received without any other processing, except pyrrole, which was distilled under reduced pressure before use. All other chemicals and reagents were of analytical grade and prepared with distilled water.

Synthesis of the FP/PEG/PPy nanocomposite

FP/PEG/PPy nanocomposite was synthesized using a chemical method. FP (2 cm × 4 cm) was added to a 30 mL aqueous solution containing PEG (2 mL) and pyrrole (0.390 mL). After evenly mixing this and letting it stand for 30 min, a 0.32 mol/L $FeCl_3$ solution (10 mL) was added as an oxidant and reacted for 12 hours at room temperature. The FP/PEG/PPy nanocomposite obtained was washed with water and alcohol several times and dried at room temperature. The preparation of FP/PEG and FP/PPy was similar to the preparation of FP/PEG/PPy but without the addition of pyrrole or PEG in the preparation solution.

Characterization and analysis

The surface morphology of FP, FP/PPy, and FP/PEG/PPy, were observed under a field emission scanning electron microscope (FE-SEM) HITACHI S-4800. The images were taken using a secondary electron detector at 5 kV accelerating voltage. Fourier transform infrared (FT-IR) spectra were recorded as KBr pellets on an EQUINOX-55 Bruker spectrometer. A spectral range of 4,000 cm^{-1} to 370 cm^{-1} was analyzed in transmittance mode. The number of scans was 32, at a resolution of 1 cm^{-1}.

Adsorption experiments

Adsorption experiments were performed by placing the same amount of FP/PEG, FP/PPy and FP/PEG/PPy into 8 mL of a Cr(VI) solution with a concentration of 100 mg/L. The amount of unabsorbed Cr(VI) ions in solution was estimated spectrophotometrically at 540 nm by the 1,5-diphenyl carbazide method (Velempini *et al.* 2017). All experiments were performed in triplicate and the average value was used. The Cr(VI) removal percentage (%) was calculated using the difference between the initial concentration and the equilibrium concentration:

$$\%\text{removal} = \frac{C_0 - C_e}{C_0} \times 100$$

where C_0 and C_e are the initial and equilibrium concentrations of Cr(VI), respectively.

Electro-assisted desorption of Cr(VI)

Electro-assisted desorption was carried out by chronoamperometry. After adsorption in 8 mL of a Cr(VI) solution with a concentration of 100 mg/L for 24 hours, FP/PEG/PPy (2 cm × 4 cm) was used as the work electrode and

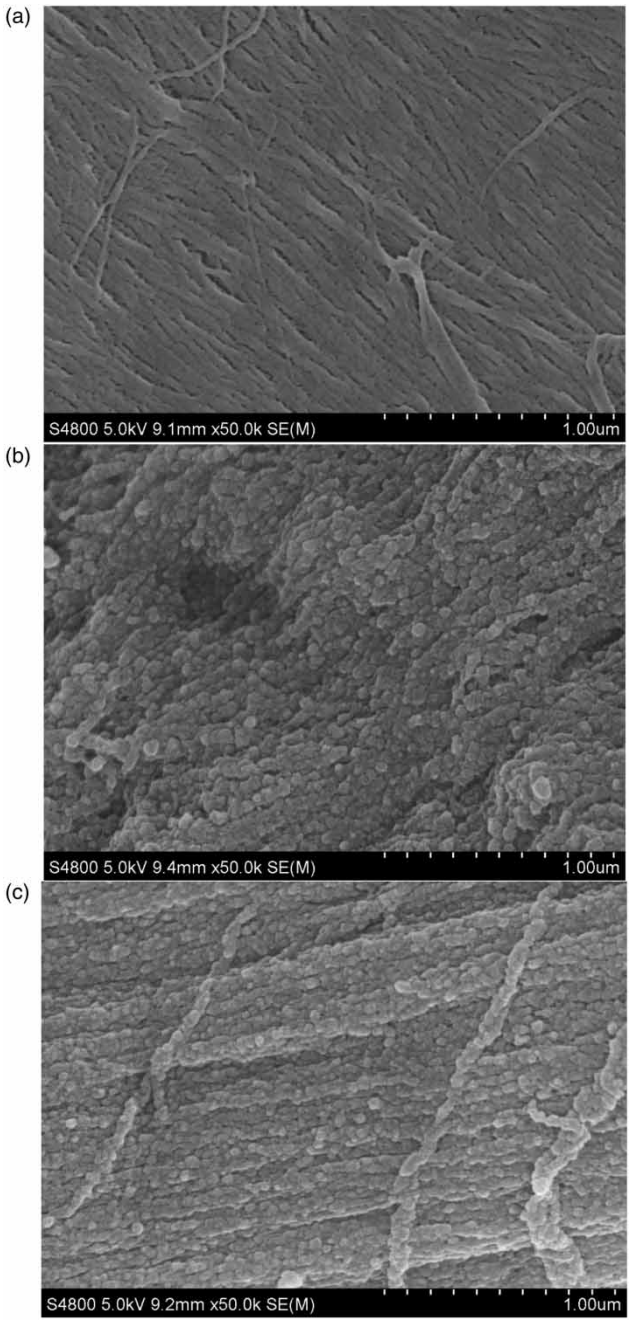

Figure 1 | FE-SEM of (a) FP; (b) FP/PPy; (c) FP/PEG/PPy at a magnification of ×50,000.

placed in a three-electrode cell with a saturated calomel electrode (SCE) as the reference electrode and Pt as the counter electrode. The desorption process was carried out with an applied potential of −1.0 V on FP/PEG/PPy in 25 mL of 0.02 M $NaHCO_3$. The auxiliary electrochemical function was evaluated by the content of Cr(VI) in the electrolyte.

Photo-assisted desorption of Cr(VI)

Photo-assisted desorption was evaluated using FP/PEG/PPy, which had been adsorbed in a Cr(VI) solution with a concentration of 100 mg/L for 24 hours. The desorption process was carried out in 25 mL of 0.02 M $NaHCO_3$ with and without illumination by a 300 W Xe arc lamp (Beijing Perfectlight, PLS-SXE300C). The Cr(VI) concentration was measured every 30 min. All trials were run in triplicate, and the average value was used.

RESULTS AND DISCUSSION

Structure and morphology analysis

FP shows a smooth surface with interconnected cellulose nanofibers (Figure 1(a)). The pyrrole monomer can be adsorbed on FP and polymerized by oxidizing agent. As shown in Figure 1(b), there are cauliflower-like structures and many defects on the surface of FP/PPy. The boundaries of these PPy platelets are defects, which lead to uneven distribution and instability of the composite. PEG can act as a surfactant or crosslinking agent, reducing the particle size of PPy and binding the particles together. As shown in Figure 1(c), the particle size decreased with the addition of PEG, and a more compact structure was obtained. Moreover, the surface arrangement of FP/PEG/PPy was more regular than FP/PPy. As shown in Figure 2, PEG may play a guiding role in the chemical synthesis of FP/PEG/PPy. The pyrrole monomer was polymerized along the cellulose nanofibers direction. As a benefit, FP/PEG/PPy not only offered a uniform microstructure but also enhanced its mechanical strength.

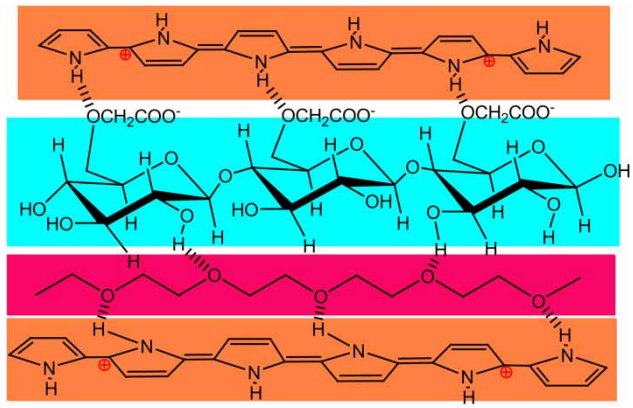

Figure 2 | Network structure formed between FP, PEG and PPy through hydrogen bonding and electrostatic interactions.

FT-IR spectra analysis

The FT-IR transmittance spectra of FP, FP/PPy, and FP/PEG/PPy are shown in Figure 3. The bands at 1,057 cm^{-1}, 1,162 cm^{-1}, and 1,112 cm^{-1} were assigned to the stretching vibration of the C-O bands of the primary alcohol, the secondary alcohol and the secondary alkyl ether, respectively. These are characteristic absorption peaks of cellulose (Lay *et al.* 2016; Zhou *et al.* 2017). These disappeared after being decorated by PEG and PPy, meaning that the alcoholic hydroxyl group of FP reacted directly with PPy and PEG. The strong bands at 1,600 cm^{-1} and 765 cm^{-1} are characteristic of the C = C vibration and = C-N plane vibration, illustrating the structure of the aromatic ring of PPy (Li *et al.* 2016; Li *et al.* 2017). The absorption peak of 1,349 cm^{-1} assigned to the C-N single bond also indicated the existence of PPy (Nascimento *et al.* 2016). The 2,802 cm^{-1} peak related to the retractable vibration of methylene, indicating the existence of PEG (Ji *et al.* 2018).

Batch adsorption experiments

As shown in Figure 4, FP and FP/PEG do not show an obvious adsorption capacity for Cr(VI). In the FP/PPy complex, PPy is the main adsorption component for Cr(VI) and almost 52% Cr(VI) was adsorbed from solution in 180 min. By comparison, 58% Cr(VI) was removed by FP/PEG/PPy in 180 min. With the addition of PEG, the oxygen atoms in PEG can form hydrogen bonds with the H(N-H) of PPy to build a network structure that can provide suitable spaces and a high adsorption area for Cr(VI). In addition, the introduction of PEG not only improves the toughness and strength of FP/PEG/PPy but also enhances the electrical conductivity of FP/PEG/PPy to a certain extent (Gao

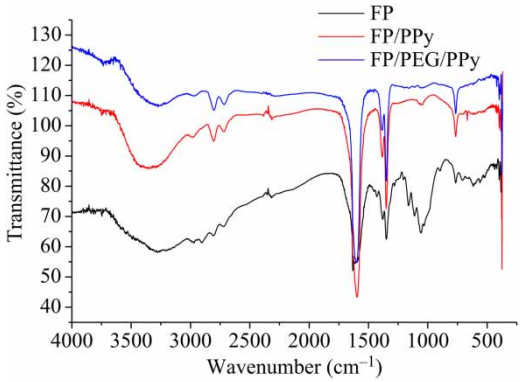

Figure 3 | FT-IR spectra of FP, FP-PPy and FP-PEG-PPy.

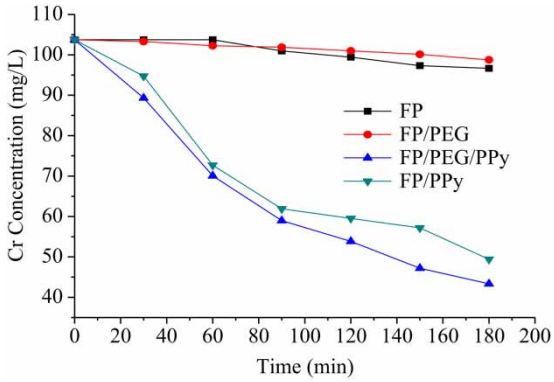

Figure 4 | Adsorption capacity of FP, FP/PEG, FP/PPy and FP/PEG/PPy.

et al. 2017). Higher electrical conductivity is necessarily for the modulation of potential of FP/PEG/PPy. Thus, the electro-assisted desorption process can be enhanced.

Electro-assisted desorption of Cr(VI)

Electro-assisted desorption was performed by applying a −1.0 V potential on FP/PEG/PPy in 0.02 M $NaHCO_3$ for 10 min, while FP/PEG/PPy was immersed directly in 0.02 M $NaHCO_3$ as a control. As shown in Figure 5(a), the current-time curve shows that this electro-assisted process can be complete in 50 seconds. The amount of Cr(VI) released with an applied potential of −1.0 V was approximately six

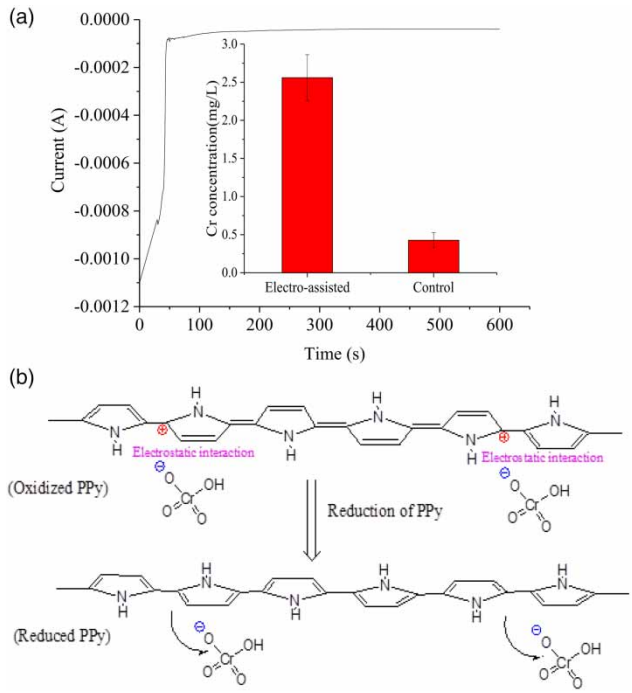

Figure 5 | Electro-assisted desorption of FP/PEG/PPy.

times that with no potential applied (as shown in the inset of Figure 5(a)). Under a reduction potential of −1.0 V, PPy can change from being in an oxidation state to a reduction state. The disappearance of positive sites led to the release of negatively charged Cr(VI) (Figure 5(b)). Meanwhile, the reduction of PPy can cause an increase in its hydrophobicity, which is also advantageous for the removal of Cr(VI) (Otero 2013).

Photo-assisted desorption of Cr(VI)

The oxidized PPy can produce a positive charge site per three or four pyrrole units. The positively charged sites in the PPy are easily attacked by the nucleophilic reagent, leading to the overoxidation of PPy. Overoxidation is directly related to the concentration of the nucleophilic reagent (Li & Qian 2000). Elution with a high concentration of alkaline solution greatly affects its regeneration efficiency (Ballav *et al.* 2012; Bhaumik *et al.* 2012). Due to the high photostability of PPy, photo-assisted alkaline elution can reduce its dependence on the alkali concentration (Wang *et al.* 2014a). Photo-assisted desorption was investigated using a xenon lamp and a low-concentration eluent (0.02 M $NaHCO_3$). The effect of light on the desorption of Cr(VI) was mainly reflected in two aspects: the temperature effect and the chemical state transition.

First, FP/PEG/PPy strongly absorbs light, leading to an increase in temperature (Huang *et al.* 2017). As shown in the inset of Figure 6(a), the temperature of FP/PEG/PPy increased from 24.2 °C to 59.4 °C over 5 min illumination, while the temperature of FP only increased from 24.2 °C to 38.5 °C. An increase in temperature is beneficial to the diffusion of Cr(VI) at the time of desorption and improves the efficiency of desorption. As shown in Figure 6(a), with the increase in temperature, the concentration of released Cr(VI) in the solution also gradually increased.

Second, FP/PEG/PPy can absorb photons and produce photonic electrons and holes. Photo-assisted elution was investigated using a low concentration of $NaHCO_3$ (0.02 M). As shown in Figure 6(b), at the same temperature, the desorption ability of FP/PEG/PPy under light was higher than that in the dark. After desorbing for 150 min, the spent FP/PEG/PPy composite released more Cr(VI) with the aid of light. The concentration of Cr(VI) in eluent reached 0.84 mg/L with light in 150 min, while only 0.31 mg/L was achieved in the dark. The result suggests that photonic electrons can induce the chemical transition of PPy from the oxidation state to the reduction state, releasing negative Cr(VI).

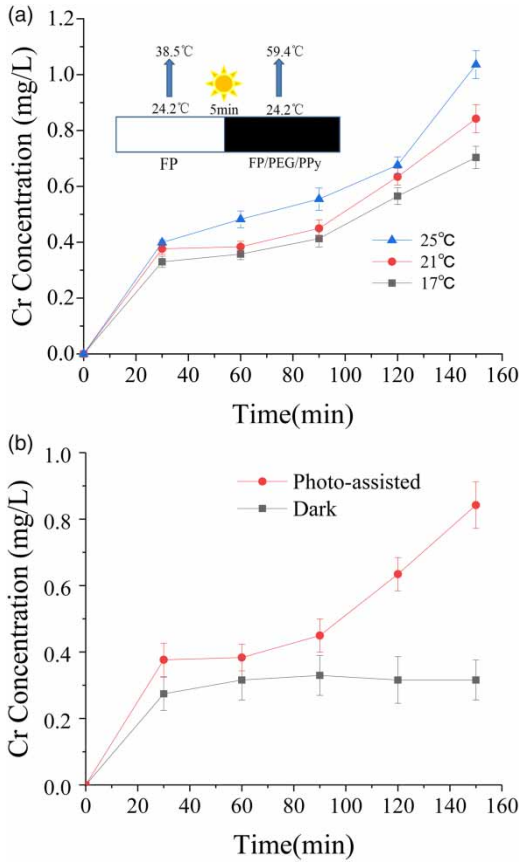

Figure 6 | Photo-assisted desorption of FP/PEG/PPy.

Meanwhile, produced photonic electrons can also cause the reduction of Cr(VI) to Cr(III). PEG, as an electron donating component, can eliminate the oxidizing holes. Alkoxy radicals produced initially by hole oxidation may also be beneficial to reduction (Wang *et al.* 2014b; Miller & Chuang 2016). As shown in Figure 7, in addition to Cr(VI),

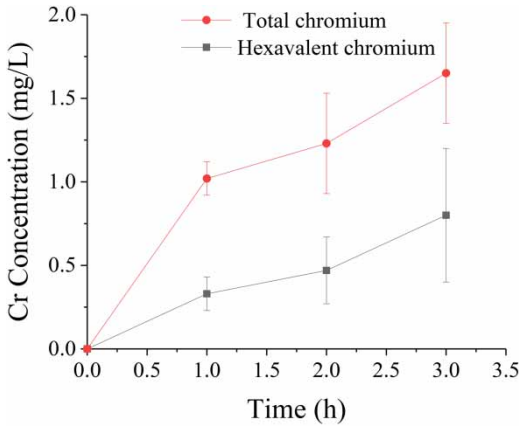

Figure 7 | Hexavalent chromium and total chromium analysis in eluent.

there was an amount of Cr(III) in the eluting fluid. The desorption process was associated with the partial reduction of adsorbed Cr(VI) to Cr(III) species by photonic electrons or electron-rich PPy moieties (Bhaumik *et al.* 2011).

CONCLUSION

In this paper, FP/PEG/PPy was synthesized and tested as an adsorbent of Cr(VI). It was found that the addition of PEG can help improve the dimensional uniformity, the arrangement of the microstructure and the mechanical properties of the whole material. FP/PEG/PPy was used as a PPy-based adsorbent for Cr(VI). It was found that photo- and electro-assisted processes can play a positive role in the regeneration process. Compared with other Cr(VI) adsorbents, photo/electric sensitive FP/PEG/PPy not only has the advantage of high adsorption capacity and low cost, but also has the ability of using clean energy (light energy and electrical energy), which can reduce reliance on an elution reagent and avoid secondary pollution to environment.

ACKNOWLEDGEMENTS

This work was financially supported by the Open Project of the Key Laboratory of Degraded and Unused Land Consolidation Engineering, the Ministry of Land and Resources, Fundamental Research Funds for the Central Universities (No. 310829161015, No. 310829162014 and No. 310829165007) and the Science and Technology Research and Development Program of Shaanxi Province (No. 2012GY2-35).

REFERENCES

Aroua, M. K., Zuki, F. M. & Sulaiman, N. M. 2007 Removal of chromium ions from aqueous solutions by polymer-enhanced ultrafiltration. *Journal of Hazardous Materials* **147** (3), 752–758.

Ballav, N., Maity, A. & Mishra, S. B. 2012 High efficient removal of chromium (VI) using glycine doped polypyrrole adsorbent from aqueous solution. *Chemical Engineering Journal* **198**, 536–546.

Bermúdez, Y. G., Rico, I. L. R., Guibal, E., de Hoces, M. C. & Martín-Lara, M. Á. 2012 Biosorption of hexavalent chromium from aqueous solution by *Sargassum muticum* brown alga. Application of statistical design for process optimization. *Chemical Engineering Journal* **183**, 68–76.

Bhaumik, M., Maity, A., Srinivasu, V. V. & Onyango, M. S. 2011 Enhanced removal of Cr (VI) from aqueous solution using polypyrrole/Fe_3O_4 magnetic nanocomposite. *Journal of Hazardous Materials* **190** (1), 381–390.

Bhaumik, M., Maity, A., Srinivasu, V. V. & Onyango, M. S. 2012 Removal of hexavalent chromium from aqueous solution using polypyrrole-polyaniline nanofibers. *Chemical Engineering Journal* **181**, 323–333.

Bishnoi, N. R., Bajaj, M., Sharma, N. & Gupta, A. 2004 Adsorption of Cr (VI) on activated rice husk carbon and activated alumina. *Bioresource Technology* **91** (3), 305–307.

Chiha, M., Samar, M. H. & Hamdaoui, O. 2006 Extraction of chromium (VI) from sulphuric acid aqueous solutions by a liquid surfactant membrane (LSM). *Desalination* **194** (1–3), 69–80.

Choi, D., Zhu, C., Fu, S., Du, D., Engelhard, M. H. & Lin, Y. 2017 Electrochemically controlled ion-exchange property of carbon nanotubes/polypyrrole nanocomposite in various electrolyte solutions. *Electroanalysis* **29** (3), 929–936.

Chowdhury, D., Paul, A. & Chattopadhyay, A. 2005 Photocatalytic polypyrrole-TiO_2-nanoparticles composite thin film generated at the air-water interface. *Langmuir* **21** (9), 4123.

Dantas, T. N. D. C., Neto, A. A. D., Moura, M. C. P. D. A., Neto, E. L. B. & Telemaco, E. D. P. 2001 Chromium adsorption by chitosan impregnated with microemulsion. *Langmuir* **17** (14), 4256–4260.

Gang, D., Hu, W., Banerji, S. K. & Clevenger, T. E. 2001 Modified poly (4-vinylpyridine) coated silica gel. Fast kinetics of diffusion-controlled sorption of chromium (VI). *Industrial & Engineering Chemistry Research* **40** (4), 1200–1204.

Gao, F., Zhang, N., Fang, X. & Ma, M. 2017 Bioinspired design of strong, tough, and highly conductive polyol-polypyrrole composites for flexible electronics. *ACS Applied Materials & Interfaces* **9** (7), 5692–5698.

Ghorbani, M. & Eisazadeh, H. 2013 Removal of COD, color, anions and heavy metals from cotton textile wastewater by using polyaniline and polypyrrole nanocomposites coated on rice husk ash. *Composites Part B: Engineering* **45** (1), 1–7.

Goshu, I. V., Tsarev, Y. V. & Kostrov, V. V. 2009 Kinetics of chromium (VI) adsorption from model solutions on iron oxide. *Russian Journal of Applied Chemistry* **82** (5), 801–804.

Huang, X., Yu, Y. H., de Llergo, O. L., Marquez, S. M. & Cheng, Z. 2017 Facile polypyrrole thin film coating on polypropylene membrane for efficient solar-driven interfacial water evaporation. *RSC Advances* **7** (16), 9495–9499.

Ji, F., Zhang, K., Li, J., Gu, Y., Zhao, J. & Zhang, J. 2018 A dual pH/magnetic responsive nanocarrier based on pegylated Fe_3O_4 nanoparticles for doxorubicin delivery. *Journal of Nanoscience & Nanotechnology* **18** (7), 4464.

Karthik, R. & Meenakshi, S. 2015 Chemical modification of chitin with polypyrrole for the uptake of Pb (II) and Cd (II) ions. *International Journal of Biological Macromolecules* **78**, 157–164.

Lay, M., Méndez, J. A., Delgado-Aguilar, M., Bun, K. N. & Vilaseca, F. 2016 Strong and electrically conductive

nanopaper from cellulose nanofibers and polypyrrole. *Carbohydrate Polymers* **152**, 361–369.

Levankumar, L., Muthukumaran, V. & Gobinath, M. B. 2009 Batch adsorption and kinetics of chromium (VI) removal from aqueous solutions by *Ocimum americanum* L. seed pods. *Journal of Hazardous Materials* **161** (2), 709–713.

Li, Y. & Qian, R. 2000 Electrochemical overoxidation of conducting polypyrrole nitrate film in aqueous solutions. *Electrochimica Acta* **45** (11), 1727–1731.

Li, C., Chen, N., Zhao, Y., Li, R. & Feng, C. 2016 Polypyrrole-grafted peanut shell biological carbon as a potential sorbent for fluoride removal: sorption capability and mechanism. *Chemosphere* **163**, 81–89.

Li, Y., Bober, P., Trchová, M. & Stejskal, J. 2017 Polypyrrole prepared in the presence of methyl orange and ethyl orange: nanotubes versus globules in conductivity enhancement. *Journal of Materials Chemistry C* **5** (17), 4236–4245.

Lim, C. W., Song, K. & Kim, S. H. 2012 Synthesis of PPy/silica nanocomposites with cratered surfaces and their application in heavy metal extraction. *Journal of Industrial and Engineering Chemistry* **18** (1), 24–28.

Miller, D. D. & Chuang, S. S. 2016 The effect of electron-donating groups and hydrogen bonding on H_2S capture over polyethylene glycol/amine sites. *The Journal of Physical Chemistry C* **120** (2), 1147–1162.

Nascimento, T. A., Dutra, F. V. A., Pires, B. C., Tarley, C. R. T., Mano, V. & Borges, K. B. 2016 Preparation and characterization of a composite based on polyaniline, polypyrrole and cigarette filters: adsorption studies and kinetics of phenylbutazone in aqueous media. *RSC Advances* **6** (69), 64450–64459.

Omraei, M., Esfandian, H., Katal, R. & Ghorbani, M. 2011 Study of the removal of Zn (II) from aqueous solution using polypyrrole nanocomposite. *Desalination* **271** (1), 248–256.

Otero, T. F. 2013 Reactions drive conformations. Biomimetic properties and devices, theoretical description. *Journal of Materials Chemistry B* **1** (31), 3754–3767.

Pérez-Candela, M., Martín-Martínez, J. & Torregrosa-Maciá, R. 1995 Chromium (VI) removal with activated carbons. *Water Research* **29** (9), 2174–2180.

Rammelt, U., Bischoff, S., El-Dessouki, M., Schulze, R., Plieth, W. & Dunsch, L. 1999 Semiconducting properties of polypyrrole films in aqueous solution. *Journal of Solid State Electrochemistry* **3** (7–8), 406–411.

Velempini, T., Pillay, K., Mbianda, X. Y. & Arotiba, O. A. 2017 Epichlorohydrin crosslinked carboxymethyl cellulose-ethylenediamine imprinted polymer for the selective uptake of Cr (VI). *International Journal of Biological Macromolecules* **101**, 837–844.

Wampler, W. A., Basak, S. & Rajeshwar, K. 1996 Composites of polypyrrole and carbon black: 4. Use in environmental pollution abatement of hexavalent chromium. *Carbon* **34** (6), 747–755.

Wang, Q., Wang, J., Lv, G., Wang, F., Zhou, X., Hu, J. & Wang, Q. 2014a Facile synthesis of hydrophilic polypyrrole nanoparticles for photothermal cancer therapy. *Journal of Materials Science* **49** (9), 3484–3490.

Wang, W., Ye, M., He, L. & Yin, Y. 2014b Nanocrystalline TiO_2-catalyzed photoreversible color switching. *Nano Letters* **14** (3), 1681–1686.

Xing, J. Y., Zhu, C. Z., Chowdhury, I., Tian, Y. H., Du, D. & Lin, Y. H. 2018 Electrically switched ion exchange based on polypyrrole and carbon nanotube nanocomposite for the removal of chromium(VI) from aqueous solution. *Industrial & Engineering Chemistry Research* **57** (2), 768–774.

Yusof, A. M. & Malek, N. A. N. N. 2009 Removal of Cr (VI) and As (V) from aqueous solutions by HDTMA-modified zeolite Y. *Journal of Hazardous Materials* **162** (2), 1019–1024.

Zhang, S., Shao, Y., Liu, J., Aksay, I. A. & Lin, Y. 2011 Graphene–polypyrrole nanocomposite as a highly efficient and low cost electrically switched ion exchanger for removing ClO_4–from wastewater. *ACS Applied Materials & Interfaces* **3** (9), 3633–3637.

Zhao, J., Li, Z., Wang, J., Li, Q. & Wang, X. 2015 Capsular polypyrrole hollow nanofibers: an efficient recyclable adsorbent for hexavalent chromium removal. *Journal of Materials Chemistry A* **3** (29), 15124–15132.

Zhou, J., Lü, Q. F. & Luo, J. J. 2017 Efficient removal of organic dyes from aqueous solution by rapid adsorption onto polypyrrole–based composites. *Journal of Cleaner Production* **167**, 739–748.

First received 9 January 2018; accepted in revised form 29 May 2018. Available online 11 June 2018